Correlation of Magnetic Fluctuations and Edge Transport in the Doublet III Tokamak

N. Ohyabu, G. L. Jahns, R. D. Stambaugh, and E. J. Strait
GA Technologies Inc., San Diego, California 92138
(Received 17 October 1986)

A clear correlation between incoherent magnetic fluctuations and transport in the outer region of the plasma was observed in a set of Doublet III beam-heated discharges which experienced repetitive transitions between a poor-confinement phase and an improved-confinement phase. The fluctuations and associated transport are consistent with a model based on an assembly of saturated microtearing modes.

PACS numbers: 52.55.Fa, 52.25.Fi, 52.30.−q

Observations of improved energy confinement ("*H*-mode" discharges) in tokamaks[1-3] suggest that edge confinement plays a critical role in the determination of global energy confinement, i.e., longer edge confinement leads to longer core confinement. Plausible theoretical models have been advanced to explain this relationship,[4,5] and acceptance of this viewpoint shifts the problem of confining a fusion plasma to one of understanding and improving the confinement at the plasma edge.

To this end, this Letter reports observations from the Doublet III tokamak wherein the level of magnetic turbulence is directly correlated with (and thus may be responsible for) edge transport. The turbulence is low frequency (5–50 kHz) and broadband,[6] and increases with β_p, as previously observed on the ISX-B tokamak.[7] The correlation here is established more directly than in previous experiments[6-10] because the observed incoherent magnetic-fluctuation amplitude abruptly changes simultaneously with transitions into and out of the *H* mode. A model based on microtearing modes will be shown to be consistent with the observed turbulence with regard to the spatial amplitude dependence, frequencies, magnitude of heat transport, and the existence of a temperature threshold to the *H* mode as observed on the ASDEX tokamak.[1]

Magnetic fluctuations are detected by two arrays (poloidal and toroidal) of Mirnov coils that sense the poloidal magnetic field. They are located just inside the Doublet III vacuum vessel [see Fig. 1(a)] which acts as a perfectly conducting shell in the frequency range of interest ($f > 2$ kHz). Each coil is inside a stainless-steel shield that excludes electrostatic pickup while reducing electromagnetic signals by only 10% at 25 kHz. The highest measurable frequency, 50 kHz, is determined by the maximum data-acquisition rate.

In Doublet III ($B_T < 2.4$ T, $I_p < 1$ MA, $R = 1.44$ m, $a = 0.4$ m), as with other tokamaks, it is found that as neutral-beam heating power is increased in discharges defined by a material limiter, the global energy-confinement time τ_E decreases (*L* mode).[1,11] If, however, the plasma is well diverted, the confinement deterioration is more modest, and τ_E is typically a factor of 2 higher than limiter discharges at high beam-heating levels. In the Doublet III poloidal divertor configuration, neutral-particle sources are localized in the divertor region, whereas a limited discharge exhibits larger sources, mainly near the limiter. *Marginally diverted* discharges are intermediate, with recycling at both limiter and divertor regions, and are observed to undergo repetitive transitions between an *L* phase and an *H* phase[1] (the average τ_E is not as long as that of fully diverted discharges, but is better than that of limiter discharges). The transitions in marginally diverted discharges provide an ideal situation for the study of the differences between *L*- and *H*-mode transport.

Figure 1(a) shows an example of the outer magnetic-flux surfaces of a marginally diverted discharge ($B_t < 1.1$ T, $q = 2.6$, $\beta_p = 0.75$, $b/a = 1.35$, $a = 0.39$ m). Figures 1(b)–1(d) show successive time expansions of relevant diagnostic signals from this discharge. The D_α light intensity indicates the relative amount of particle recycling and hence edge particle transport since external sources (e.g., gas puff, chamber wall) are slowly varying in time. In Fig. 1(c), there are two intervals of low D_α intensity, which is the signature of *H*-mode confinement. (The D_α intensity from the divertor also decreases, and so this drop is more than just a shift in recycling location.) Observations on the ASDEX and the PDX tokamak have established that global energy confinement improves when the edge-particle transport drops.[1,2] An improvement in global energy confinement can also be inferred from the soft-x-ray traces in Fig. 1: The signal labeled SXR-11 looks just outside the $q = 1$ radius and so it rises at the sawtooth crash and then decays. During *H*-phase time intervals [e.g., from times t_2 to t_3 in Fig. 1(c) and 1(d)], the decay rate immediately becomes very slow, indicating the reduction of heat transport in this internal region.

Figure 1(d) also shows that the Mirnov-probe signal amplitude abruptly decreases at the onset of the *H* phase (time t_2) and increases again at the transition back to the *L* phase (time t_3). The synchronous change of magnetic-fluctuation amplitude with the change in edge confinement (e.g., D_α signal) establishes a clear correlation between these quantities.

Observed properties of the magnetic fluctuations are shown in Fig. 2. Frequency spectra of the Mirnov-probe signal (integrated to give $\tilde{b}$), Fig. 2(a), are incoherent

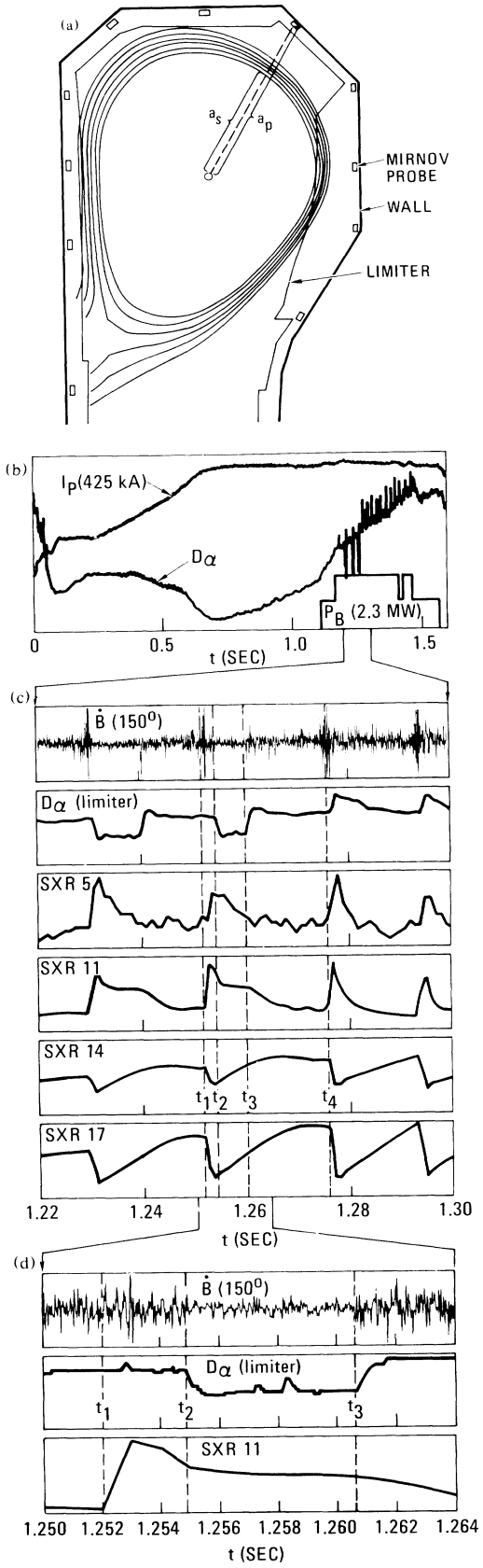

above about 5 kHz and generally decrease with frequency in both H and L phases. Signals from other poloidal locations have widely varying amplitudes, and it is found that this is due principally to the variation in the distance from plasma to probe; Fig. 2(b) shows that the signal amplitude strongly decreases with the distance ratio a_p/a_s, as defined in Fig. 1(a). Figure 2(c) shows the coherence[12] between pairs of toroidally displaced probes at outside midplane locations for frequency bands 5 kHz wide. The coherence drops below the 95% confidence level within 30° to 90°, demonstrating again the incoherent nature of the fluctuations.

A model to account for these features is that the plasma edge region contains a collection of microtearing modes.[13,14] (Similar observtions in the ISX-B tokamak were attributed to resistive ballooning modes.[7]) A microtearing mode is driven by the temperature gradient at a frequency of order of the electron diamagnetic frequency, ω^*. For the case above, $\omega^*/2\pi \sim 13$ kHz if $T \approx 200$ eV and $[(1/n)(\partial n/\partial x)]^{-1} \approx 5$ cm. The stability condition $v_e^* < \omega_e^*$ can be reexpressed as $T > C \times [(nB_T/m)(T/\nabla T)]^{2/5}$, where C is a numerical coefficient, predicting a temperature threshold above which the microtearing mode is stable. This is consistent with the observed temperature threshold for the H-mode transition in the ASDEX tokamak. For discharges such as are shown in Fig. 1, the predicted threshold is about 200 eV, a reasonable value. It may be noted in Fig. 1(c) that the two L-H transitions follow closely a sawtooth crash, possibly because the extra heat from the center warms the edge to a temperature over the threshold. Bolometric measurements show increasing radiated power in the edge region during H phase, apparently cooling the edge until it eventually makes a transition back to the L phase.

The island structure of a single microtearing mode of poloidal mode number m would give a magnetic field $\tilde{b} \sim (a_p/a_s)^{-m-1}$ in the region between plasma and wall in a cylindrical approximation. An assembly of modes would have a radial falloff progressively dominated by the lowest m components with significant amplitude at the plasma surface. Noncircularity would cause a poloidal asymmetry. The signal amplitudes in Fig. 2(b) are fitted well by $\tilde{b} \sim (a_p/a_s)^{-8.75 \pm 1.67}$, indicating a lower bound of $m \simeq 8$ of modes present. The data are for

FIG. 1. (a) Cross section of the Doublet III tokamak showing location of Mirnov (magnetic) probes, and magnetic-flux surfaces for a discharge with H-to-L transitions. a_p and a_s correspond to distances from the plasma center to Mirnov probe and plasma surface, respectively. (b) Time traces from a beam-heated discharge. (c) A time expansion during beam heating of a Mirnov-probe signal ($\dot{B}$), D_α light, and soft-x-ray views from edge to center (SXR-5, $r/a_s \sim 0.9$; SXR-11, $r/a_s \sim 0.5$; SXR-14, $r/a_s \sim 0.2$; SXR-17, $r/a_s \sim 0.0$). (d) A further time expansion of an L-to-H-to-L transition.

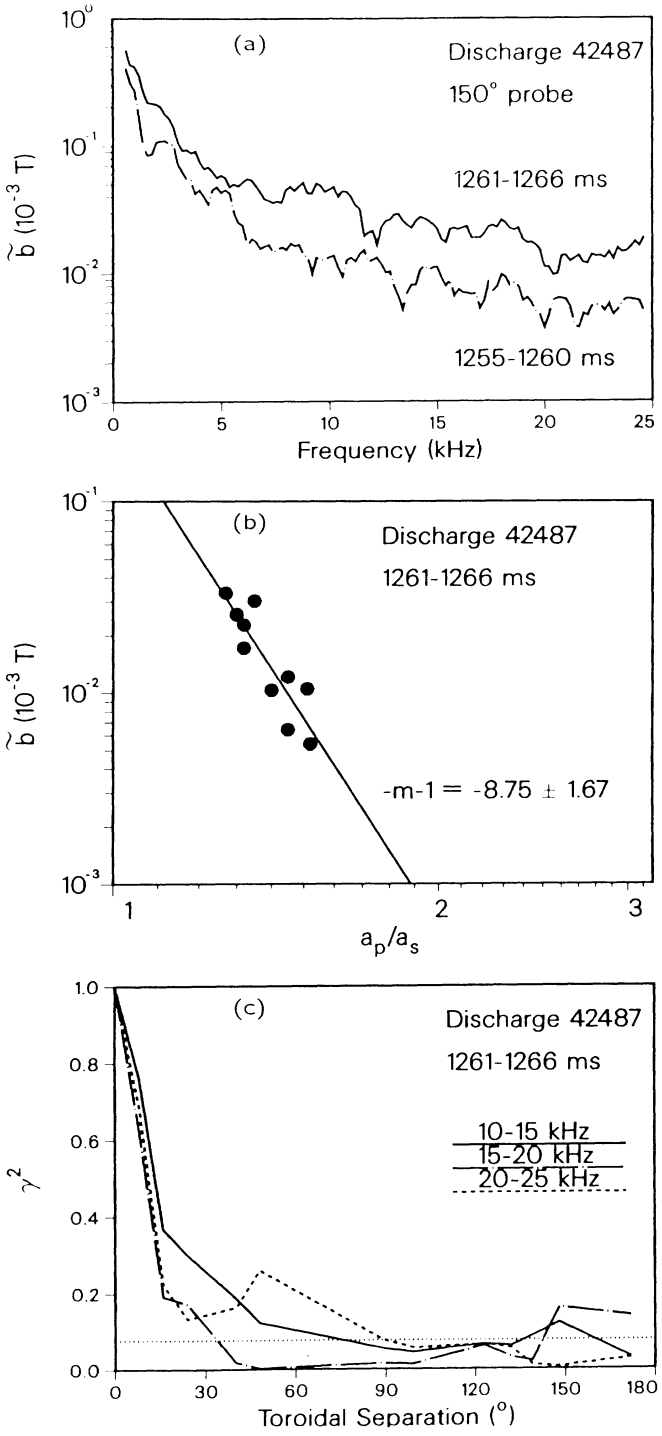

FIG. 2. (a) Frequency spectra of the time-integrated Mirnov probe signal for an H-phase and an L-phase time interval from Fig. 1(c). (b) Dependence of signal amplitude in the 10–15-kHz band on the probe/surface distance ratio a_p/a_s. (c) Coherence (γ^2) of outer midplane probe signals as a function of their toroidal angular separation. The dotted horizontal line is the level of 95% confidence of coherence.

the 10–15-kHz band; there is no significant difference for higher-frequency bands. The scatter in the data reflected in the uncertainty in the exponent is consistent with about a factor of 2 poloidal amplitude variation which may arise from noncircular effects. It is concluded that the data are well described by a collection of island structures of poloidal mode number 8 and higher.

The radial falloff measured above can be used to estimate the magnitude of the magnetic fluctuations in the plasma edge region. For $m=8$, $\tilde{b}$ at the plasma surface is about a factor of 7 larger than the value at the probe. A normalized value of $|\tilde{b}|/B_T$ at the plasma surface is $\simeq 2\times 10^{-4}$ for the L phase in Fig. 2. This indicates a full island width as large as 2.0 cm. For comparison, the distance between neighboring rational surfaces, e.g., $\frac{8}{3}$ and $\frac{10}{4}$, is about 1.3 cm, so that overlapped islands with

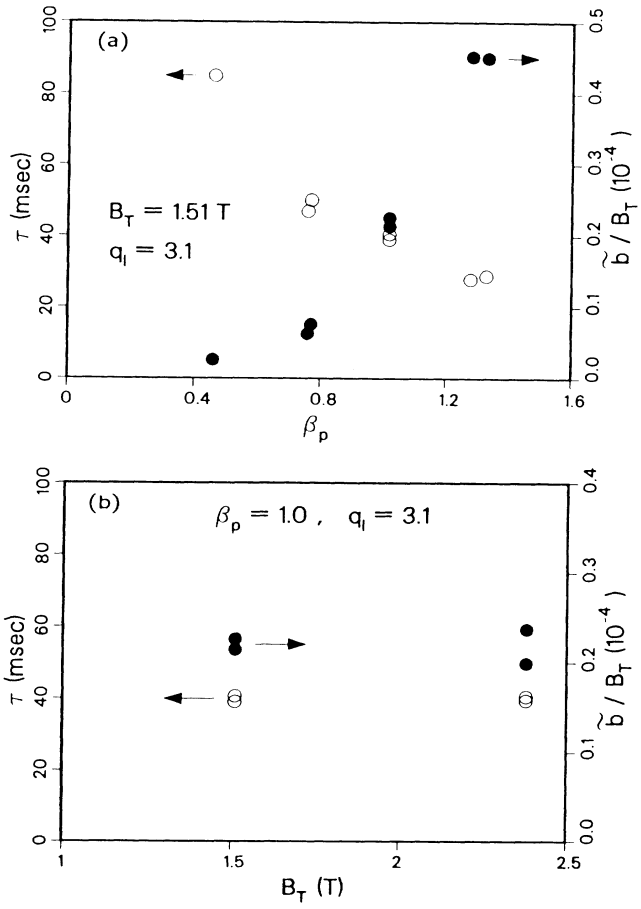

FIG. 3. Variation of global confinement time (open circles) and normalized magnetic-fluctuation amplitude from the inner midplane probe for the 10–15-kHz band (solid circles) for a set of discharges satisfying the conditions κ fixed, a_p/a_s fixed, and q_l fixed. (a) Change in confinement time and fluctuation amplitude as β_p is varied at constant toroidal magnetic field. (b) Variation of confinement time and fluctuation amplitude with toroidal magnetic field when β_p is constant.

enhanced electron thermal transport are expected.[15] (It should be noted that overlapped islands do not directly predict enhanced *particle* transport.) The effective thermal diffusivity can be estimated from $(|\tilde{b}|/B_T)^2 \times v_e qR$ (from Rechester and Rosenbluth[16]), where v_e is the electron thermal velocity, to be 2 m^2/sec for $T_e = 200$ eV, comparable to transport-code estimates of the edge thermal diffusivity. The hypothesis of overlapped multiple-island layers is also qualitatively consistent with the observed incoherent nature of detected magnetic signals.

Returning to the deterioration of confinement with increased heating power, the influence of edge magnetic turbulence on global confinement depends on the additional processes linking edge and global energy transport.[4,5] This makes quantitative predictions of scaling difficult, although one would expect that increasing turbulence would result in progressively enhanced transport and deteriorating energy confinement. A regression analysis of beam-heated tokamak confinement data has shown that $\tau_E \propto P_{\rm tot}^{-0.5} I_p^{1.0}$ (L-mode scaling), where $P_{\rm tot}$ is the total input power and I_p is the plasma current.[11] This can be reexpressed in terms of the poloidal beta as $\tau_E \propto \beta_p^{-1}$, with no dependence on the toroidal field B_T. Figure 3(a) demonstrates that the normalized fluctuation amplitude increses with β_p as τ_E decreases.[17] The data in the figure are restricted to circular discharges limited on the inside limiter so that a_p/a_s is fixed at 1.11 to eliminate any effect from the strong dependence of the probe signal on probe-plasma distance, except for outward flux surface shifts with increasing β_p that would tend to *reduce* the inner-wall probe signal. Similarly, only data with fixed q_l ($=3.1$) are considered to avoid any effect of q profile on mode location. The few data meeting these criteria with β_p fixed show no dependence of $\tilde{b}/B_T$ or τ_E on B_T in Fig. 3(b). Thus, the parametric variation of the observed fluctuation amplitude is qualitatively consistent with L-mode scaling.

In conclusion, low-frequency incoherent magnetic-fluctuation amplitudes are observed to change synchronously with edge transport in transitions between H and L confinement phases. The fluctuations exhibit the incoherence, frequency range, and radial-amplitude decrease expected of an assembly of microtearing modes with $m \geq 8$. Microtearing modes are predicted to be stable above a threshold temperature in agreement with ASDEX observations. Measured fluctuation amplitudes indicate island structures of size sufficient to enhance edge transport. To the extent that edge transport influences global confinement, the observed magnetic turbulence is a viable candidate for the origin of L-mode scaling, as demonstrated by the increase of fluctuation amplitudes with increasing β_p.

The authors thank Dr. D. Overskei and Dr. R. Dominguez for their encouragement and valuable comments. This work was sponsored by the U.S. Department of Energy under Contract No. DE-AC03-84ER51044.

[1]F. Wagner *et al.*, Phys. Rev. Lett. **49**, 1408 (1982).
[2]S. M. Kaye *et al.*, J. Nucl. Mater. **121**, 115 (1984).
[3]N. Ohyabu *et al.*, Nucl. Fusion **25**, 49 (1985).
[4]H. P. Furth, Bull. Am. Phys. Soc. **30**, 1386 (1985).
[5]N. Ohyabu, J. K. Lee, and J. de Grassie, Nucl. Fusion **26**, 593 (1986).
[6]S. J. Zweben *et al.*, Phys. Rev. Lett. **42**, 1270 (1979).
[7]B. A. Carreras *et al.*, Phys. Rev. Lett. **50**, 503 (1983).
[8]P. A. Duperrex *et al.*, Phys. Lett. **106A**, 133 (1984).
[9]J. J. Ellis, A. A. Howling, A. W. Morris, and D. C. Robinson, in *Proceedings of the Tenth International Conference on Plasma Physics and Controlled Nuclear Fusion Research, London, 1984* (IAEA, Vienna, 1985), Vol. 1, p, 373.
[10]S. K. Guharay, K. Kawahata, and N. Noda, J. Nucl. Mater. **128&129**, 325 (1984).
[11]S. M. Kaye and R. J. Goldston, Nucl. Fusion **25**, 65 (1985).
[12]J. S. Bendat and A. G. Piersol, *Random Data: Analysis and Measurement Procedures* (Wiley-Interscience, New York, 1971), p. 32.
[13]N. T. Gladd, J. F. Drake, C. L. Chang, and C. S. Liu, Phys. Fluids **23**, 1182 (1980).
[14]R. R. Dominguez, M. Rosenberg, and C. S. Chang, Phys. Fluids **24**, 472 (1981).
[15]P. H. Rebut and M. Brusati, Plasma Phys. Controlled Fusion **28**, 113 (1986).
[16]A. B. Rechester and M. N. Rosenbluth, Phys. Rev. Lett. **40**, 38 (1978).
[17]E. J. Strait *et al.*, in *Proceedings of the Eleventh European Conference on Controlled Fusion and Plasma Physics, Aachen, West Germany, 1983* (European Physical Society, Petit-Lancy, Switzerland, 1983), p. 59.